Numerical and experimental modal analysis of the reed and pipe of a clarinet

Matteo Facchinetti, Xavier Boutillon, Andrei Constantinescu

Numerical and experimental modal analysis of the reed and pipe of a clarinet[a)]

Matteo L. Facchinetti
Laboratoire de Mécanique des Solides and Laboratoire d'Hydrodynamique, CNRS-École Polytechnique, 91128 Palaiseau Cedex, France

Xavier Boutillon[b)]
Laboratoire d'Acoustique Musicale, CNRS-Université Paris 6-Ministère de la Culture, 11 rue de Lourmel, 75015 Paris, France

Andrei Constantinescu
Laboratoire de Mécanique des Solides, CNRS-École Polytechnique, 91128 Palaiseau Cedex, France

A modal computation of a complete clarinet is presented by the association of finite-element models of the reed and of part of the pipe with a lumped-element model of the rest of the pipe. In the first part, we compare modal computations of the reed and the air inside the mouthpiece and barrel with measurements performed by holographic interferometry. In the second part, the complete clarinet is modeled by adjoining a series of lumped elements for the remaining part of the pipe. The parameters of the lumped-resonator model are determined from acoustic impedance measurements. Computed eigenmodes of the whole system show that modal patterns of the reed differ significantly whether it is alone or coupled to air. Some modes exhibit mostly reed motion and a small contribution of the acoustic pressure inside the pipe. Resonance frequencies measured on a clarinet with the mouthpiece replaced by the cylinder of equal volume differ significantly from the computed eigenfrequencies of the clarinet taking the actual shape of the mouthpiece into account and from those including the (linear) dynamics of the reed. This suggests revisiting the customary quality index based on the alignment of the peaks of the input acoustical impedance curve.

I. INTRODUCTION

The clarinet is usually considered as the association of a linear resonator, the pipe, and a nonlinear excitor, the reed, subject to the air flow from the mouth. Alternatively, one can consider the air column and the reed as a linear system subject to nonlinear boundary conditions. This is the approach retained in this article where the reed is considered as a linear mechanical system coupled to the pipe and where the interaction with the player is not treated. Nonlinear phenomenon such as the interaction between the reed and the jet across the reed-slit, the contact forces between the reed and the lay, and the interaction between the reed and the player's lip will be included in a subsequent piece of work as nonlinear boundary conditions to the normal modes that are described here. Humidity of the reed and the player's lip also have a damping role which is not considered in this modal analysis of a pipe coupled to a (dry) reed.

Acoustical studies of the clarinet have so far represented the mouthpiece of a wind instrument by its equivalent volume. This study goes beyond this approximation and presents the three-dimensional distribution of the pressure in the upper part of the instrument.

Studies of the pipe of the clarinet have traditionally been expressed in the frequency domain and were based on measurements or computations of input acoustic impedance. However, numerical simulations of this instrument operate in the time domain and are usually based on the reflection function of the pipe. Recent experimental studies have adopted the time domain approach with direct measurements of this reflection function. Abundant literature extensively covers these subjects: for general presentations, see Refs. 1–4.

Studies of the reeds are far less extensive and the mechanical behavior of cane is still subject to discussion. The simplest reed model, a spring, is implicitly used by reedmakers when they rate them by their so-called ''strength,'' which corresponds to the mechanical compliance. Experimental studies have proposed values for the compliance of the reed.[1,5,6] Associated with various models of the pipe and excitation, this model has been used in numerical simulations which were successful in describing basic features of the dynamics of clarinet-like system.[7–9] Music-oriented algorithms have also been proposed in which the values of the parameters describing the excitor and the resonator are adjusted in order to obtain realistic sounds instead of accurately describing their mechanical behavior.[10,11] However, this model is obviously insufficient to describe quality-based criteria: otherwise all reeds in a given commercial box (with

[a)]Part of this work was presented in ''Application of modal analysis and synthesis of reed and pipe to numerical simulations of a clarinet,'' invited paper at the 140th meeting of the ASA, Newport Beach, CA, December 2000 [J. Acoust. Soc. Am. **108**, 2590(A)], in ''Étude modale d'une clarinette,'' Proceedings of the Colloque National en Calcul de Structures, Giens, France, May 2001, and in ''Modal analysis of a complete clarinet,'' Proceedings of the International Conference on Acoustics, Rome, Italy, September 2001.

[b)]Electronic mail: boutillon@lms.polytechnique.fr; present address: Laboratoire de Mecanique des Solides, Ecole Polytechnique, 91128 Palaiseau Cedex, France.

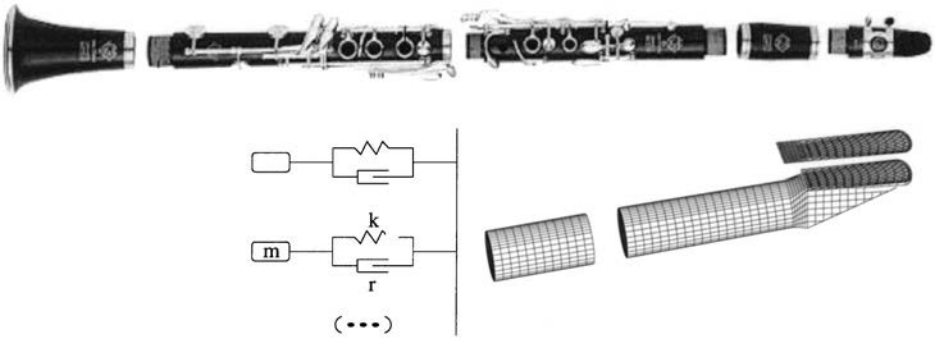

FIG. 1. The clarinet: its parts and their respective models (not to scale).

similar strength) would suit a given player, but this is not the case.

The next modeling step is the single-degree-of-freedom oscillator. Although some simulation algorithms[12] have been very successful in producing realistic sounds,[13,14] this is not sufficient in itself to assert the physical validity of a model. One degree of freedom is not sufficient to account for criteria such as reed quality. Stewart and Strong[15] and Sommerfeld and Strong[16] used a refined model of the reed as a nonuniform beam. In the latter study, the pipe was only slightly simplified compared to a real clarinet and the player's air column (including the lungs) was also taken into account. There is no fundamental difference between this simulation and those based on a simple oscillator model for the reed since the interaction with the rest of the system is averaged along the beam. The beam model is needed if one wants to take into account the curved shape of the mouthpiece on which the reed beats during large amplitude motions. Gazengel[17] derived a simple oscillator model from a beam equation. In his time-domain simulation, the mass of the oscillator is recalculated at each time step as a function of the position of the reed, introducing by this means the nonlinear behavior of the reed contact.

Modeling the reed as a continuous system is the current state of research. Several examples of modal analysis of clarinet reeds with holographic interferometry have been presented in conferences over the recent years,[18–20] but never published. One example of finite-element modeling based on measurements of the mechanical properties of cane has been reported.[21] Another (unpublished) pioneering study has been done by Pinard and Laine when they were students at the École Polytechnique (France). The experimental modal analysis and the finite-element modeling of isolated reeds that are presented in the following are a development of this unpublished work. To our knowledge, no model of the reed as a continuous system in association with the air column has been proposed.

The model proposed here is aimed at overcoming several limitations of previous approaches. Besides giving a means to review the approximations of the classical model, this new approach is also a first step toward numerical simulations of the instrument based on modal projection[22,23] rather than on propagation schemes represented by reflection functions.

The different parts of a clarinet—reed, mouthpiece, barrel, upper and lower parts of the pipe, bell—are shown in Fig. 1 together with their respective models. Fluid and solid finite-element models (FEM) for the reed and the beginning of the pipe and a lumped elements model for the main part of the pipe are used.

The work presented here begins with the modal analysis of the isolated reed. In each subsequent section, another element of the model is added, finally resulting in a complete instrument. In addition, the modes of the reed associated with the mouthpiece and barrel are compared with the results of experimental modal analysis.

II. THE REED

A. Construction of the numerical model

Establishing a finite element model requires the determination of the geometry of the reed, the choice of a constitutive law, the determination of the mechanical parameters, as well as the appropriate boundary conditions.

A series of three reeds have been measured. The thickness of each reed was measured with a coordinate measuring machine (Mitutoyo EURO-M 574 and Johansson Saphir 7 were used). Approximately 200 points, arbitrarily chosen on the reed surface, have been measured [Fig. 2(a)]. The geometrical data for the model are interpolated from the measured values. Interpolation between measured points was done by using a fourth-order polynomial, resulting in and giving the thickness map shown in Fig. 2(b). The reed is assumed to be symmetrical with regard to its longitudinal axis.

The shape of the reed was measured using a high precision optical projector (Macro Dynascope 5D, by Vision Engineering with Metronics Quadra-Check 4000 interpolating software) with the results shown in Fig. 2(c). The precision of the geometrical measurements of the reed can be estimated to $\approx 2\ \mu$m.

Reeds are made out of cane which is considered here as a purely elastic, transversely isotropic, homogeneous material. Viscosity and plasticity, related to energetic losses, have been neglected at this step of the analysis. The homogeneity hypothesis will be analyzed a posteriori in Sec. V. In the current state of knowledge, we have found no other plausible description that could be expressed quantitatively.

A discussion of losses in cane has been given lately by Marandas *et al.*[24] and Obataya and Norimoto.[25] The former found out that dry cane is viscoelastic and turns viscoplastic when wet. This implies that static tests on wet cane are not appropriate to measure Young's moduli. Obataya proposed values of the quality factor Q of the order of magnitude of

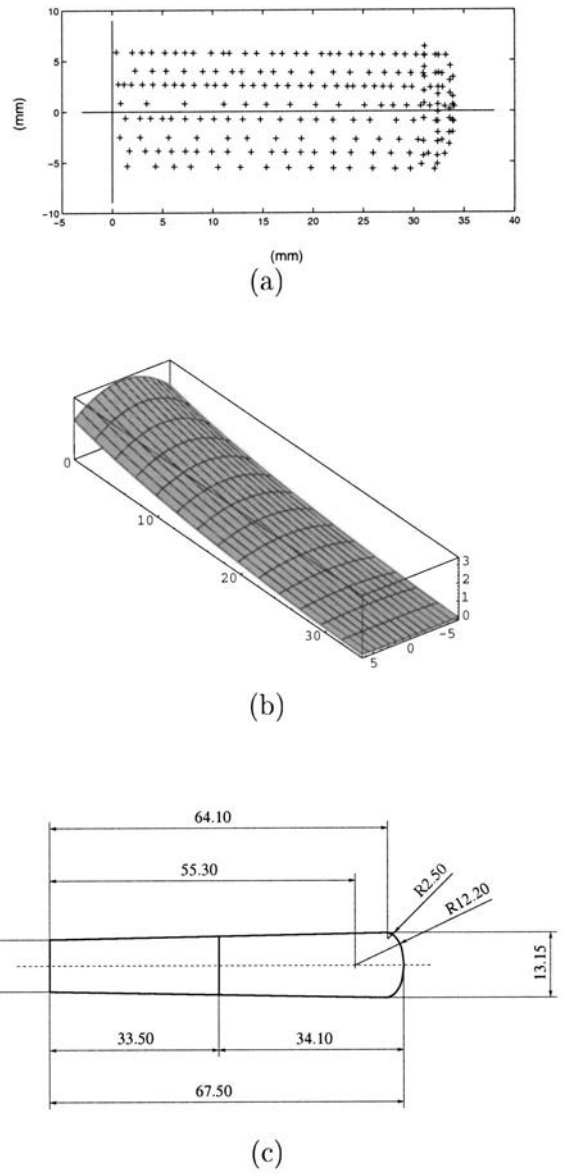

FIG. 2. Geometry of the reed, with dimensions in mm: (a) points actually measured, (b) interpolated thickness, (c) estimated contour.

100 varying with frequency, relative humidity, and internal state of cane. Since only individual modes of the reed are considered here losses can be ignored. They would need to be taken into account in modeling the actual dynamics of the instrument.

Under these assumptions, five parameters are needed to describe the material: density ρ_s, longitudinal and transverse Young's moduli E_L and E_T, transverse to longitudinal shear modulus G_{LT}, and longitudinal-transverse Poisson ratio ν_{LT}. The values adopted here are given in Table I. The values for ρ_s, E_L, and ν_{LT} were obtained by Pinard and Laine and result from static measurements on a piece of dry cane given by a reed maker. Obataya and Norimoto give roughly the same value for the main Young's modulus E_L of dry cane in the frequency that is relevant here (2–6 kHz). Their measurements show that this value decreases linearly with the relative humidity level (RH), E_L decreasing by around 30% for a variation of 100% in RH. The other parameters were

TABLE I. Material properties for dry cane used in reeds, as given by Pinard and Laine.

Density	$\rho_s = 450$ kg/m^3
Longitudinal Young modulus	$E_L = 10\,000$ MPa
Transverse Young modulus	$E_T = 400$ MPa
Shear modulus	$G_{LT} = 1300$ MPa
Poisson ratio	$\nu_{LT} = 0.22$

also obtained by Pinard and Laine. Their work has been pioneering in several respects. In particular, they were the first to match eigenfrequencies and modal patterns of reeds obtained by holographic interferometry with those obtained with a finite-element model.

As boundary condition, we consider the reed rigidly clamped on the section corresponding to the ligature and having a stress-free boundary elsewhere.

B. Computed eigenmodes

This model has been implemented on a standard PC (450 MHz, 250 Mbyte RAM, Linux) using linear Love–Kirchoff plate elements in the CAST3M finite-element code. The first modes of a reed are presented in Fig. 3. A classification of the modes is needed for referencing and an attempt is made here. Since modal patterns with closed modal lines have not been encountered, it is intuitively appealing to label the modes according to the number of intersections between the nodal lines and the edges of the reed. For the symmetric reed considered here, a mode is labeled *LnTm*. "*L*" stands for longitudinal and the first index *n* is the number of intersections of nodal lines with the edge(s) parallel to the main axis. Such nodal lines include the one imposed by the boundary condition at the ligature. "*T*" stands for transverse and the index *m* is the number of intersections of the nodal lines with the tip edge of the reed. Modes appear in an order which can be expected ($L1T0$, $L1T1$, $L2T0$, $L1T2$, $L2T1$), given the larger flexibility in the direction transverse to the reed and the thickness distribution.

The generalized mass of a mode is:

$$m = \mathbf{u}^T \mathbf{M}_s \mathbf{u}, \tag{1}$$

where $\mathbf{u}$ represents the reed displacement for the mode and $\mathbf{M}$ is the mass matrix of the reed. For a unit value of the maximum displacement in each mode, the modal masses are 7, 0.35, 0.47, 0.063, and 0.094 mg for the $L1T0$, $L1T1$, $L2T0$, $L1T2$, and $L2T1$ modes, respectively. Along with modal patterns, these values establish a comparison between modes. These mass values can also be compared to the order of magnitude of the real mass of the moving reed. At the tip of the reed, the thickness is about 1/10 mm and the width 13 mm. For a density $\rho_s = 450\,\mathrm{kg\,m^{-3}}$, the mass of a moving portion of the reed of length l (in mm) is $(0.59 \times l)$ mg.

III. MODAL COMPUTATION OF THE REED ASSOCIATED WITH MOUTHPIECE AND BARREL

This section analyzes how the dynamics of the reed is influenced by air loading and provides a comparison between results given by the model and experiments presented in Sec.

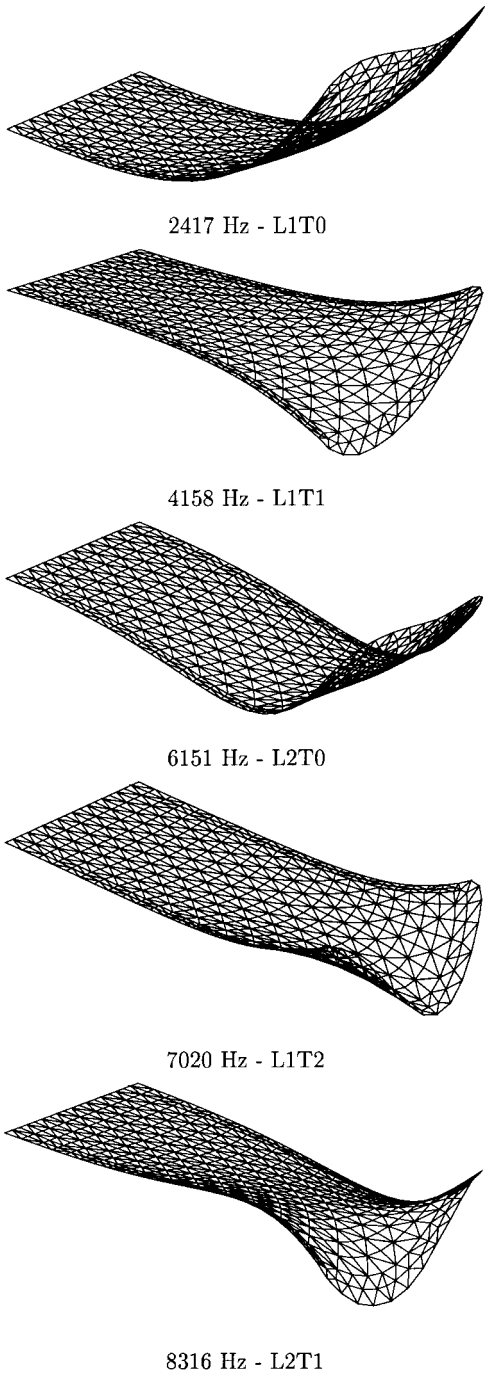

FIG. 3. First five computed modes of an isolated reed. Modes are labeled according to the number of modal lines perpendicular to the main axis (*Ln*) and parallel to it (*Tm*).

II. The system considered now is composed of the reed, the mouthpiece, and the barrel and is represented using a coupled fluid–solid model.

A. Numerical model

The full model of reed, mouthpiece, and open barrel is shown in Fig. 4. The internal shape of the mouthpiece (a Selmer HS*) has been carefully measured by means of the coordinate measuring machine used for the reed. The barrel is considered as a cylindrical bore with a diameter of 15 mm. The air volume inside the mouthpiece and the barrel is modeled with linear tetrahaedric and prismatic finite elements of compressible elastic fluid.

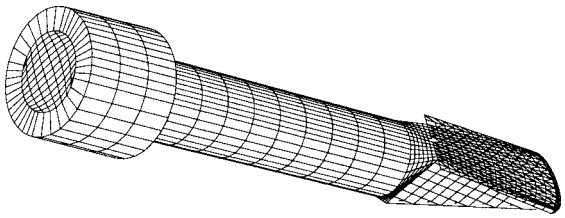

FIG. 4. Reed and volume of air inside the mouthpiece mounted on an open barrel.

The acoustic pressure at points of the open air surfaces is considered to be zero. The normal derivative of the acoustic pressure on the walls of the mouthpiece and the barrel, corresponding to air flow, is also set to zero. The boundary condition coupling the reed and the mouthpiece involves the stress in the solid and the velocity of the fluid and will be given explicitly in the following.

The eigenvalue problem for a coupled solid–fluid system is expressed in the continuous formulation by the following:[26]

$$\mathrm{div}\,\mathbf{C}\nabla\mathbf{u}-\omega^2\rho_s\mathbf{u}=0, \tag{2}$$

$$\mathrm{div}\,\frac{1}{\rho_f}\boldsymbol{\nabla} p+\omega^2\frac{1}{c^2\rho_f}p=0, \tag{3}$$

where p represents the acoustic pressure in the fluid. The densities of solid and fluid are ρ_s and ρ_f, respectively. The speed of sound is c, the angular frequency of the motion is ω, and $\mathbf{C}$ denotes the elasticity matrix of the solid.

The boundary conditions coupling the fluid and the solid parts are

$$\boldsymbol{\sigma}\cdot\mathbf{n}=-p\mathbf{n}, \tag{4}$$

$$\frac{\partial p}{\partial\mathbf{n}}=\rho_f\omega^2\mathbf{u}\cdot\mathbf{n}, \tag{5}$$

where $\mathbf{n}$ represents the unit vector normal to the solid surface and $\boldsymbol{\sigma}=\mathbf{C}\nabla\mathbf{u}$ the stress tensor.

In order to formulate these equations as a standard eigenvalue problem, a new variable $\pi=-(1/\omega^2)p$ must be introduced.[26] The equations and boundary conditions become

$$\mathrm{div}\,\mathbf{C}\nabla\mathbf{u}-\omega^2\rho_s\mathbf{u}=0, \tag{6}$$

$$\mathrm{div}\,\frac{1}{\rho_f}\boldsymbol{\nabla}\pi-\frac{1}{c^2\rho_f}p=0, \tag{7}$$

$$\omega^2\pi+p=0, \tag{8}$$

$$\boldsymbol{\sigma}\cdot\mathbf{n}=-p\mathbf{n}, \tag{9}$$

$$\frac{\partial\pi}{\partial\mathbf{n}}=-\rho_f\mathbf{u}\cdot\mathbf{n}. \tag{10}$$

To the preceding equations, we can associate the following Lagrangian $\mathcal{L}$ denoting the variational formulation of the problem:

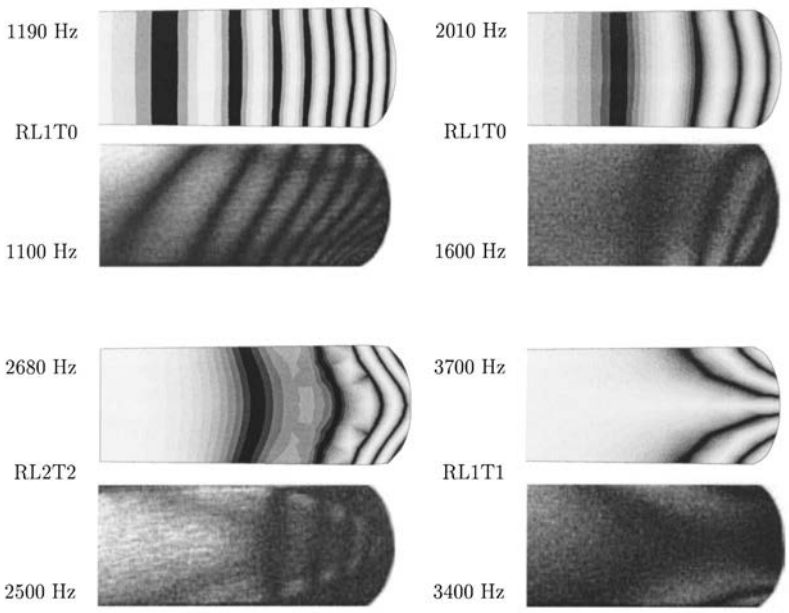

FIG. 5. Projection of four eigenmodes on the reed (see the text for labels). Top pictures: computed normalized eigenmodes of the association of a reed with mouthpiece and barrel. In this representation, a cyclic gray scale produces fringes of equal differences in normal displacement, allowing a comparison with the modal patterns observed experimentally. Bottom pictures: modal patterns measured by holographic interferometry on one good reed mounted on the mouthpiece attached to the barrel. The resonance is not very sharp owing to damping, hence the rounded eigenfrequencies. The photographed section of the reed does not have the same height between the various experiments and the simulations.

$$\mathcal{L}=\frac{1}{2}\int_{\Omega_s}\nabla\mathbf{u}\mathbf{C}\nabla\mathbf{u}\,dv+\frac{1}{2}\int_{\Omega_f}\frac{1}{\rho_f c^2}p^2\,dv - \omega^2\left(\frac{1}{2}\int_{\Omega_s}\rho_s\mathbf{u}^2\,dv-\frac{1}{2}\int_{\Omega_f}\frac{1}{\rho_f c^2}(\boldsymbol{\nabla}\pi)^2 dv - \int_{\Omega_f}\frac{1}{\rho_f c^2}p\,\pi\,dv-\int_{\partial\Omega}\pi\boldsymbol{\sigma}\cdot\mathbf{n}\,ds\right), \tag{11}$$

where Ω_s and Ω_f represent the solid and fluid volumes, respectively, and $\partial\Omega$ represents the boundary between these volumes.

Finally, the problem is expressed in its discrete form by the following eigenvalue problem:

$$\left(\begin{bmatrix}\mathbf{K}_s & 0 & 0\\ 0 & \mathbf{K}_f & 0\\ 0 & 0 & 0\end{bmatrix}-\omega^2\begin{bmatrix}\mathbf{M}_s & 0 & -\mathbf{N}\\ 0 & 0 & \mathbf{K}_f\\ -\mathbf{N}^T & \mathbf{K}_f^T & -\mathbf{M}_f\end{bmatrix}\right)\begin{bmatrix}\mathbf{u}\\ p\\ \pi\end{bmatrix}=\begin{bmatrix}0\\ 0\\ 0\end{bmatrix},$$

where $\mathbf{K}_s$ (respectively, $\mathbf{K}_f$) and $\mathbf{M}_s$ (respectively, $\mathbf{M}_f$) are rigidity and mass matrices of the solid (respectively, fluid) part of the system and $\mathbf{N}$ is the operator corresponding to the coupling boundary condition (10) related to the normal vector $\mathbf{n}$. Details of the derivation can be found in Ref. 26.

B. Experimental modal analysis

An experimental modal analysis on reeds by means of holographic interferometry was performed in order to check the validity of the numerical model of the reed coupled to air. Recent works have been reported in short communications.[18–20] For various reeds mounted on a mouthpiece under dry conditions Pinard and Laine observed one mode corresponding to a longitudinal flexion at around 2200 Hz; one family of modes around 3500–3700 Hz, with patterns varying from reed to reed, some of them being indicative of torsion, others being closer to flexion; and one family of modes around 5800–6000 Hz, with more complex patterns.

In measurements presented here, the reed was attached to the mouthpiece exactly as on the real instrument. Since the ligature was producing strong light reflexions, it was replaced with adhesive tape placed slightly further from the tip. A sinusoidally driven loudspeaker was placed close to the reed to excite its vibration. For determining the resonance frequencies a very thin PVDF piezoelectric film [poly(vinylidenefluoride), thickness 0.05 mm, mass 0.06 g, of which only a part was actually moving] was glued onto the lower thicker part of the reed, yielding the average deformation near the ligature. Resonance frequencies were determined using the maximum of the piezoelectric signal. The experiments were performed under natural humidity. A saturated atmosphere would have been preferable but was not possible with the interferometry equipment.

The eigenmodes were visualized by means of laser transmission interferometry. Complete details of the implementation of this classical method are described in Ref. 27. The images in Fig. 5 represent variations of equal normal-displacement of the reed. The resolution of the system is half the wavelength of the laser, approximately 0.3 μm.

The reed was measured either alone, associated with an open mouthpiece, or with the mouthpiece mounted on an open barrel. The first four measured modes shown in Fig. 5 correspond to the barrel configuration (see Fig. 4). They are compared with the corresponding computed modal patterns (see the next section for computation of the eigenmodes) on top. Results of the holographic measurements show that the maximum displacement of the reed is negligible compared to the distance between the mouthpiece and the reed at that level of excitation. Thus one can be confident that contact between the reed and the lay, which could possibly make the system nonlinear, does not occur.

TABLE II. Sensitivity analysis: changes in eigenfrequencies when mechanical characteristics of the reed and acoustical properties of the air vary. Changes are given in % for a 10% variation of each parameter.

$\Delta = 10\%$ mean values	E_L 10^4 MPa	E_T 400 MPa	G_{LT} 1300 MPa	ν_{LT} 0.22	ρ_s 450 kg m^{-3}	c 340 m s^{-1}	ρ_f 1.23 kg m^{-3}
1190 Hz	0	0	0	0	0	9.8	0
2010 Hz	2.4	0	0	0	−2.2	0.7	−0.4
2680 Hz	0.1	0	0	0	−0.2	9.6	0
3700 Hz	1.5	0	3.1	0	−4.6	0	0
4010 Hz	0.2	0	0	0	−0.2	9.3	0
4740 Hz	4.9	0	0	0	−4.8	2.7	−0.1
5280 Hz	0.6	0	0	0	−0.9	8.1	−0.1
6300 Hz	1.7	0.9	4.9	0	−6.4	3.2	0

C. Results

A comparison between computed and measured modes is displayed in Fig. 5 for the situation described by Fig. 4. In this comparison with holographic measurements, the ''ligature'' of the reed had to be placed slightly beyond its normal position. This led to a slightly more flexible reed than in the normal situation. When the reed is coupled to air, one should stress that eigenmodes concern the whole system, not just the reed. Strictly speaking, expressions such as ''reed modes'' are inappropriate and refer instead to modes for which energy is *mostly* localized in the reed. Each mode has been labeled using the notation proposed earlier. The ''*R*'' prefix indicates that we regard the result just as the *projection* of the four first eigenmodes on the reed subspace. In order to simplify the discussion, we have not attempted to label the air configuration. One can notice that the $L2T2$ pattern did not appear in the isolated reed case. One can also notice that the $L1T0$ pattern of the reed appears in the two first modes of the coupled system.

The computed modes appear in the same order as the measured ones with eigenfrequencies deviating by 10%–20% from measured resonance frequencies. The modal patterns are globally the same despite the fact that no real reed is symmetric whereas the numerical model has been chosen symmetric. As expected, the modes are mainly localized at the tip of the reed where it becomes very thin, showing the importance of a precise measurement of the geometry. Although some of the mechanical parameters come themselves from a fit between observation and computation of modes of an isolated reed, the mixed fluid–solid model can be considered as valid within the range of approximations retained here.

Real reeds have natural asymmetries due to their geometry or to nonuniform mechanical properties. One notices that the asymmetry seems stronger for the lowest mode than for any other one.

D. Sensitivity analysis

The sensitivity analysis of the eigenfrequencies to variations in mechanical parameters describing the reed and in acoustical properties of the air is presented in Table II. The air volume is that of Fig. 4. Parameters are varied by 5% above and below their average values (i.e., 10% overall) and the corresponding overall variations of eigenfrequencies are reported. The value of the Poisson ratio appears to be irrelevant. Eigenfrequencies 1190, 2680, and 4010 Hz vary linearly with the speed of sound. This is also almost the case for the mode at 5280 Hz. Without looking at the modal pattern of air pressure or reed displacement, one can infer that they correspond to '' 'air modes,'' with energy mostly localized in the (short) pipe. Conversely, the mode at 3700 Hz is not influenced by air characteristics; sensitivity to the shear modulus G_{LT} indicates that the reed is subject to torsion (see the second mode of Fig. 3) and is poorly coupled to the pipe (Fig. 6). To a lesser degree, this is also the case of the mode at 6300 Hz. The mode at 4740 reveals a $(E_L/\rho_s)^{1/2}$ dependency of the eigenfrequency. It is mostly a ''reed mode'' involving primarily a longitudinal deformation. The mode at 2010 Hz is apparently a mode in which air and reed are strongly coupled. It is interesting to notice that the transverse Young's modulus does not seem to influence any frequency. The measurement of its precise value is therefore less particularly important.

E. Evolution of the eigenfrequencies

Another way of examining how the reed is coupled to the acoustic field is to follow the evolution of the eigenfrequencies when the reed is loaded by the air volume of mouthpiece and barrel. A decrease of the eigenfrequencies and a dominance of the longitudinal flexion occurs in the eigenmodes (Fig. 7).

The frequencies of the first two modes of the {reed, mouthpiece, barrel} system are mainly imposed by the resonance of the air cavity. In both modes, the reed undergoes mainly longitudinal flexion. The frequency of the torsion mode $L1T1$ (3257 Hz for the isolated reed) does not vary

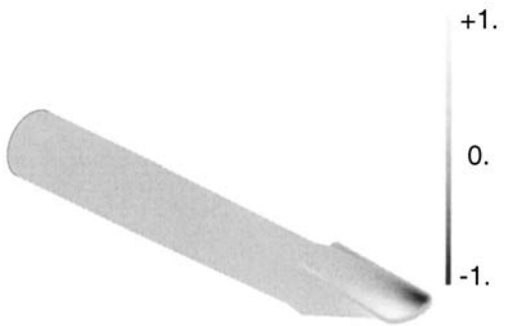

FIG. 6. Computed eigenmode at 4119 Hz in a mixed solid-air situation: acoustic pressure inside the mouthpiece and barrel.

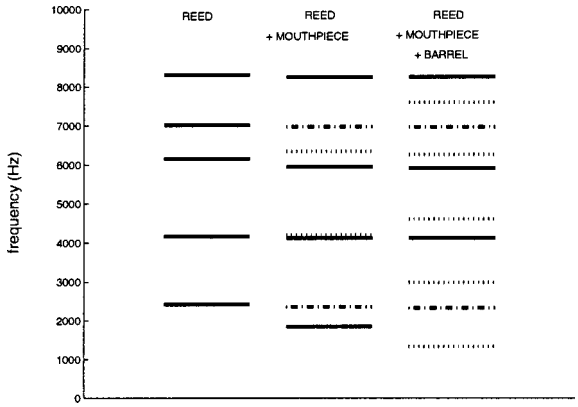

FIG. 7. Evolution of the eigenfrequencies (left scale, in hertz) when the system evolves from the isolated reed (left) to {reed+mouthpiece} (middle) and {reed+mouthpiece+barrel} (right). Black lines represent ''primary reed'' modes, dotted lines ''primary air'' modes, and dash-dot lines, ''mixed'' modes.

significantly, meaning that this mode is weakly coupled to the air cavity. The same phenomenon can be noticed for the mode $L1T2$ at 5840 Hz for the isolated reed. One can conclude from Fig. 7 and from the observation of the rather uniform pressure in the pipe at these modes (not shown here) that this mode also is weakly coupled to the pipe.

IV. MODAL COMPUTATION OF THE WHOLE CLARINET

In order to simulate the modal behavior of the complete clarinet, we have associated a finite-element model of $\approx$10 cm of pipe with lumped elements representing the rest of the pipe and matching its acoustic input impedance. This can be done since at the outlet of the barrel, the acoustic field consists essentially of plane waves. An example of acoustic pressure in the mouthpiece is represented in Fig. 8. The mode is that of a complete clarinet and corresponds to the lowest mode at 311 Hz of the medium C♯ fingering combined with the opening of the register key (see the following for the complete list of modes in this configuration). The length of mouthpiece represented here is 32 mm and corresponds to the tapered part. One can see that the acoustic waves can already be considered as plane waves within a very good approximtation.

The lumped-element oscillators (shown in generic form in Fig. 1) are coupled to the finite-element barrel by means

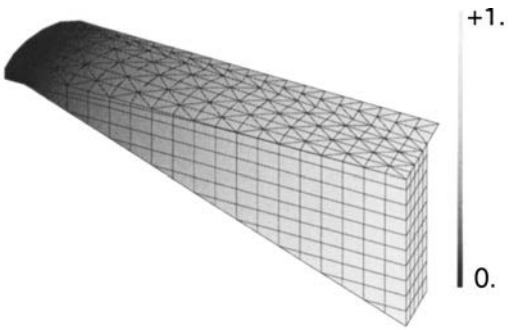

FIG. 8. Acoustic pressure inside the tip part of the mouthpiece for a 311 Hz mode of the complete clarinet. The acoustic pressure decreases monotonically from the tip to the largest section by 14%.

of a rigid plate of negligible mass, as shown in Fig. 9. The plate and the lumped-element oscillators are supposed to move only in the longitudinal axis of the instrument. The lumped elements are placed at the (virtual) junction between the barrel and the lower part of the clarinet.

It is now explained how the numerical values of the lumped elements are calculated on the basis of measurements provided by Gibiat[28] on several notes of a Noblet B♭ clarinet. Results of these measurements are supposed to represent the *input* acoustical impedance of the instrument. In order to measure this input impedance, a reference plane was defined by Gibiat *et al.* by replacing the mouthpiece with a portion of cylindrical tube of equal volume. This is the usual ''equivalent volume'' approximation which we discuss later on. Prior to matching the impedance of the lumped elements to the measured input acoustical impedance of the pipe, the latter must therefore be transported from the input plane toward the open end of the pipe. The ''transportation distance'' is equal to the length of a cylinder having the volume of the mouthpiece and the barrel.[22,29]

An oscillator is associated with each measured impedance peak. At the angular frequency ω the mechanical impedance of each elementary oscillator in Fig. 1 is

$$Z_m(\omega)=i\left(\frac{1}{m\omega}-\frac{\omega}{k+i\omega r}\right)^{-1}, \tag{12}$$

where *m, r, k* are respectively the mass, damping, and stiffness of the lumped elements.

In this ''comb-like'' association, the impedances of the oscillators add. The dual association where the admittances add is ''chain-like.'' Each elementary oscillator of Fig. 1 is a mass chained with a comb of a damper and a spring, leading to Eq. (12).

The parameters m_i, r_i, k_i of each oscillator (a tooth of the large comb) are identified by minimizing a cost functional $\mathcal{J}$ measuring the distance between computed and measured moduli and phase of the impedance:

$$\mathcal{J}=\alpha|\mathrm{Mod}(Z_{\mathrm{comp}})-\mathrm{Mod}(Z_{\mathrm{meas}})| + \beta|\mathrm{Arg}(Z_{\mathrm{comp}})-\mathrm{Arg}(Z_{\mathrm{meas}})|. \tag{13}$$

The initial values of the parameters for each oscillator are obtained by identifying each single resonance peak and the final values are obtained by running a Nelder–Mead simplex search algorithm. A comparison between the measured and the identified modulus and phase of the acoustic impedance of the lowest F fingering (E♭ heard) of the clarinet is presented in Fig. 10. The impedance represented is not the input acoustical impedance but the impedance of the lower part taken at the (virtual) junction between the barrel and the lower part of the clarinet. Therefore, the peak frequencies are not the eigenfrequencies of the instrument. The acoustical impedance represented here is the ratio of the acoustical pressure to the air velocity, normalized by ρc. The average modulus on a logarithmic scale would be 1 for an ideal long cylindrical pipe. According to Gibiat, it is less here due to internal losses, radiation, and presumably the complexity of the pipe.

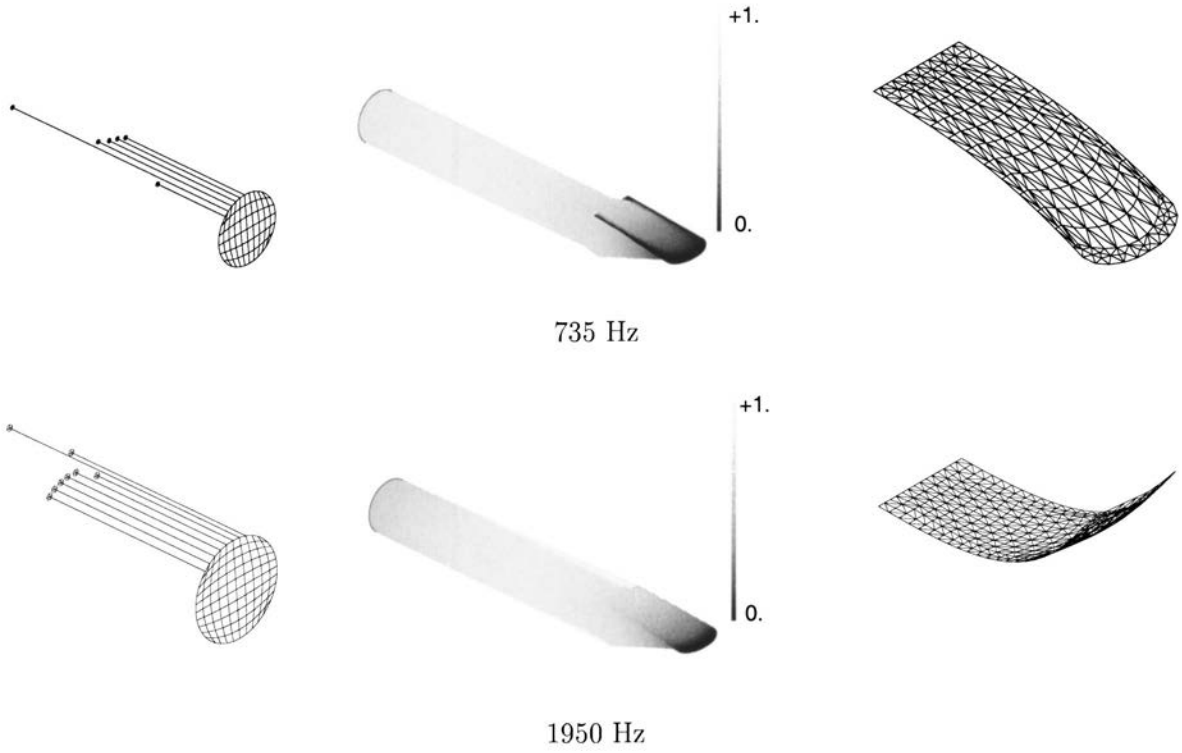

FIG. 9. Modal representation of a complete clarinet: amplitude of the motion of the lumped-element oscillators (left), air pressure in the upper part of the pipe (middle), and deformation of the reed (right). Eigenmode 2 for note treeble F# (fingering of C# medium plus opening of register key) and eigenmode 8 for note low E♭ (low F fingering).

Two eigenmodes of the complete instrument for different fingerings are shown in Fig. 9. One eigenmode has no amplitude *per se*. For each eigenmode in Fig. 9 the (relative) amplitude of the motion of the oscillators is represented by the length of a straight line extending from the plate. One notices that the pressure distribution is not uniform in the mouthpiece. Examining other similar figures reveals that the motion of the reed can differ significantly from mode to mode of a given note, even if it follows a $L1T1$ pattern. This means that, although the first modes of the isolated reed occur at significantly higher frequencies than those considered here, a single degree of freedom for the reed is not appropriate since it would not account for these differences. When the reed undergoes mostly longitudinal flexion, it is to be expected that the beam model used by several authors[15,16,30] would give comparable results.

For the low F fingering (sounding one tone lower), the first eigenfrequencies are 166, 464, 743, 1147, 1436, 1620, 1950, 2058, and 2201 Hz. They are 373, 1035, 1541, 1687, 1893, 1930, and 2309 Hz for the medium G fingering and 311, 735, 1213, 1467, 1578, 1865, and 2211 Hz for the high G♯, played with medium C♯ fingering and opening of the register key. These frequencies are represented in Fig. 11 in order to evaluate their harmonicity. Eigenfrequencies are normalized by their ratio to the theoretical musical frequency for the note under consideration (respectively, 156, 349, and 740 Hz), rounded to the nearest integer. For example, a 900 Hz eigenfrequency for note A4 (440 Hz) would be normalized by 2, nearest integer to 900/440. For this high note, the register key does not eliminate the first mode of the instrument but the sound will be locked approximately on the second mode. The lowest mode is very roughly at half the pitch of the note and is therefore normalized by the integer 2.

The sets of solid lines in Fig. 11 represent the computed eigenfrequencies listed above of the complete instrument. The sets of dashed lines are resonances of the pipe as extracted from the measurements of the input impedance of the pipe. This set represents the traditional view of the instru-

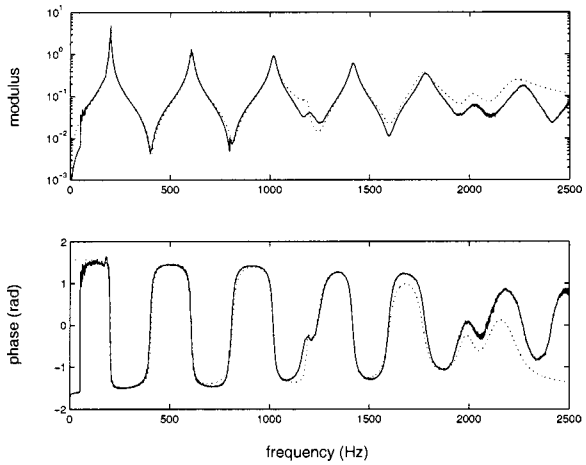

FIG. 10. Acoustical impedances (ratio of the acoustical pressure to the air velocity, normalized by ρc) for the low F note of the clarinet. Solid lines: acoustical impedance of the pipe as measured at the closed end of the pipe and transported at the (virtual) junction between the barrel and the lower part of the clarinet. Dashed lines: impedance of the set of lumped oscillators best matching the impedance of the pipe at the junction.

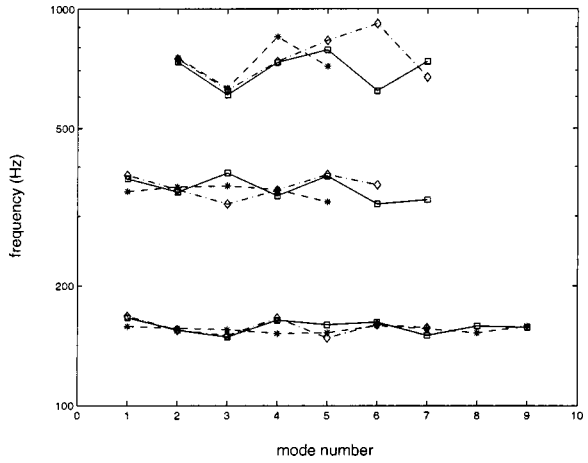

FIG. 11. Normalized eigenfrequencies (logarithmic scale) of the complete clarinet, pipe with reed (solid symbols), of the pipe with a fixed reed (dash dot), and normalized resonance frequencies measured on the pipe where the mouthpiece replaced by its equivalent volume (dashed). See the text for the definition of the normalization. Fingerings are low F, medium G, and high G♯ (medium C♯ with register key) corresponding to notes E♭ 3, F 4, and G♯ 5.

ment where the volume of the mouthpiece has been replaced by a cylindrical pipe having the same volume and closed at one end. The sets of dotted lines represent computed eigenfrequencies of the air column with a rigid boundary on the reed surface. Instead of the completely closed pipe of the traditional modeling, one assumes here a slight opening between the reed surface and the lay of the mouthpiece with a zero pressure condition.

V. DISCUSSION AND PERSPECTIVES

A. Alignment of resonances and low-frequency approximation

The traditional model of the mouthpiece is that of a cylinder of equivalent volume. Within this approximation there is no point in measuring the input acoustic impedance above a certain limit. This limit can be evaluated by the length scale at which the mouthpiece geometry differs from a cylinder. Taking as an order of magnitude for these geometrical differences a length of 1 cm is consistent with a 2.5 kHz frequency limit beyond which input acoustical impedances would begin to differ noticeably. In the approach followed in this paper, the equivalent volume approximation is abandoned and the acoustical input impedance of the pipe would keep full utility and validity up to the frequency of the first transverse mode of the pipe (13.3 kHz for the clarinet).

The cylinder of equivalent volume approximation for the mouthpiece is assumed to be correct for low frequencies. It appears in Fig. 11 that this approximation is not acceptable enough to be used in conjunction with an alignment of peaks criteria. One can see in Fig. 11 that variations in eigenfrequencies due to the model change are significant with regard to the alignment of resonances, *even at low frequencies*. In other words, the deviations from alignment in the traditional view (equivalent volume approximation) are of the same order of magnitude as the frequency shifts due to the presence of the reed and the prismatic shape of the mouthpiece.

B. Coupling of torsion modes to the air

The association of reed, mouthpiece, and a short open portion of the pipe is shown in Fig. 6. The modal acoustic pressure at an eigenfrequency of 4119 Hz is displayed in Fig. 6. In this mode, the reed undergoes torsion in a pattern very similar to the $L1T1$ mode of the isolated reed (Fig. 3). The characteristic distance of this modal deformation is significantly smaller than half the wavelength in air at that frequency ($\lambda \approx 10$ cm); the resulting acoustical short-circuit prevents any efficient coupling of the reed to the air in the mouthpiece. This explains the fairly uniform acoustic pressure for this mode, except very near to the reed. However, there are several reasons why these modes may be important in the actual playing.

First of all, the flow entering the air channel between the reed and the lay is governed by a nonlinear equation. Therefore, antisymmetric reed modes may have an influence on the global flow entering the pipe.

It has been shown that the antisymmetric reed modes are very weakly coupled to the acoustic (far)field in the clarinet. This is not to say that these modes play no role in the dynamics. Asymmetries or, better said, unevenness in the geometric or constitutive properties of reeds induce asymmetries of longitudinal reed modes and consequently an asymmetry in the local acoustical field. Due to its small relative modal mass, the torsion mode can be easily excited at a frequency different from its resonant frequency and therefore may play a significant role in the actual dynamics of the reed. The coupling factor would then be the local acoustic field. This may be an explanation for the player's experience that for different mouthpieces, the preferred reeds are also different.

This modal analysis is performed on a symmetric reed. This is not the case in reality as shown for example by the first mode in Fig. 5. The so-called torsion modes are likely to be associated in the fluid domain to a flow different from zero and therefore couple to the plane waves inside the pipe.

C. Symmetry

Experimental modal analysis shows that some reeds have strong asymmetries. Makers can be expected to be successful in controlling the symmetry of the geometry; therefore, the cause of modal asymmetries lies most probably in the lack of homogeneity of the cane used for the reed due to its natural character. Pinard, Laine, and Vach [31] examined 24 reeds, ranked by two professional players. They observed that the two reeds ranked as good and very good were symmetric whereas the poor reed had asymmetrical high modes. Based on limited sampling of reeds and players, no definite conclusion can be drawn. Intuition would suggest that asymmetry is not a desirable feature for a reed. However, we think that it might not be so.

Visualizing the lip motion in brass playing shows that lips do not move symmetrically and that this factor varies from player to player. Since brass mouthpieces are symmetric, one can conclude that the mechanical properties of lips (possibly coupled to dentition and the mouth cavity) are not symmetric for all brass players. One can hypothesize that the same is true among clarinet and saxophone players. Another

observation is that different players do not always prefer the same reeds in a given box, even for common musical tasks, style, etc., and the same clarinet and mouthpiece. A good match between a player and a reed could mean that a given asymmetry in a reed would fit well the natural asymmetry of a given player and not so well with another one. It has even been observed that a few players use reeds which fit almost none of their colleagues. It would be interesting to test these players and their preferred reeds with regard to the symmetry hypothesis.

VI. CONCLUSION

The modal analyses of reeds and of a few notes of the whole clarinet were performed. Results have shown the following points.

(1) A numerical model of cane based on the hypothesis of transverse isotropy is suited to describe modal patterns of reeds. Some of the numerical hypotheses (homogeneity, symmetry, damping) can be released but this would necessitate additional measurements.

(2) When coupled to air, the reed is subject to deformation patterns which are not always those of its own normal modes. Therefore, the normal modes of isolated reeds cannot be taken as a source for the acoustic field in the mouthpiece. Specifically, coupling must be taken into account.

(3) Torsion modes of reeds generate a strong but very localized acoustic field in the mouthpiece. It remains to be examined how this would interact with asymmetries in lower modes through the excitation process.

(4) Acoustic waves are already plane within a very good approximation in the cylindrical part of the mouthpiece. Since finite-element modeling of air is interesting insofar as the waves are not plane, the air volume in the barrel and a large proportion of that in the mouthpiece can be included in the lumped-element model, reducing significantly the computational burden.

(5) The shape of the mouthpiece and the dynamics of the reed influence the alignment of resonances in the same proportion as the misalignment derived from the customary observation of the input acoustical impedance. Therefore, the approximation of the equivalent volume is too coarse to be used when looking at harmonicity of resonances.

This study shows the need for input impedance measurements at higher frequencies than usually performed. It calls for simplified formulations of the acoustic field in the mouthpiece. The procedure outlined here could be used to test these formulations. Finally, the method paves the way for numerical simulations of the dynamics of the clarinet based on modal projection and taking into account the whole complexity of the reed.

ACKNOWLEDGMENTS

We express our gratitude to Holger Vach for his decisive help in the experimental part of this study, to Vincent Gibiat for providing us with the measurements of the acoustic input impedances and the associated software, and to Brian Katz for many language corrections.

[1] C. J. Nederveen, *Acoustical Aspects of Woodwind Instruments* (Illinois University Press (first ed. Frits Knuf Pub., Amsterdam), Dekalb, 1998 (first ed. 1968)).
[2] A. H. Benade, *Fundamentals of Musical Acoustics* (Oxford University Press, New York, 1976).
[3] J. Kergomard, ''Elementary considerations on reed-instrument oscillations,'' in *Mechanics of Musical Instruments* (Springer, New York, 1995).
[4] D. Campbell, ''Nonlinear dynamics of musical reed and brass wind instruments,'' Contemp. Phys. **40**, 415–431 (1999).
[5] J. Gilbert, ''Étude des instruments à anche simple'' (On simple reed instruments), Ph.D. thesis, Université du Maine-Le Mans, 1991.
[6] X. Boutillon and V. Gibiat, ''Evaluation of the acoustical stiffness of saxophone reeds under playing conditions by using the reactive power approach,'' J. Acoust. Soc. Am. **100**, 1178–1189 (1996).
[7] R. Schumacher, ''*Ab initio* calculations of the oscillations of a clarinet,'' Acustica **48**, 73–85 (1981).
[8] M. Mcintyre, R. Schumacher, and J. Woodhouse, ''On the oscillations of musical-instruments,'' J. Acoust. Soc. Am. **74**, 1325–1345 (1983).
[9] C. Maganza, R. Causse, and F. Laloe, ''Bifurcations, period doublings and chaos in clarinet-like systems,'' Europhys. Lett. **1**, 295–302 (1986).
[10] X. Rodet and C. Vergez, ''Nonlinear dynamics in physical models: Simple feedback-loop systems and properties,'' Comput. Music J. **23**, 18–34 (1999).
[11] J. Smith, ''Physical modeling using digital wave-guides,'' Comput. Music J. **16**, 74–98 (1992).
[12] B. Gazengel, J. Gilbert, and N. Amir, ''Time-domain simulation of single reed wind instrument—From the measured input impedance to the synthesis signal—Where are the traps?,'' Acta Acustica **3**, 445–472 (1995).
[13] E. Ducasse, ''Modelisation et simulation dans le domaine temporel d'instruments à vent a anche simple en situation de jeu'' (Time-domain model and simulation of simple-reed instruments in playing conditions), Ph.D. thesis, Université du Maine-Le Mans, 2001.
[14] E. Ducasse, ''Models of musical-instruments for sound synthesis: Application to woodwind instruments,'' J. Phys. (France) **51**, 837–840 (1990).
[15] S. Stewart and W. Strong, ''Functional-model of a simplified clarinet,'' J. Acoust. Soc. Am. **68**, 109–120 (1980).
[16] S. Sommerfeldt and W. Strong, ''Simulation of a player clarinet system,'' J. Acoust. Soc. Am. **83**, 1908–1918 (1988).
[17] B. Gazengel and J. Gilbert, ''Numerical simulations in time and frequency domains—Comparative-study, application to single-reed woodwind instruments,'' J. Phys. IV **4**, 577–580 (1994).
[18] P. Hoekje and G. Roberts, ''Observed vibration patterns of clarinet reeds,'' J. Acoust. Soc. Am. **99**, 2462(A) (1996).
[19] I. Lindevald and J. Gower, ''Vibrational modes of clarinet reeds,'' J. Acoust. Soc. Am. **102**, 3085(A) (1997).
[20] B. Richardson (private communication).
[21] D. Casadonte, ''The perfect clarinet reed? Vibrational modes of realistic clarinet reeds,'' J. Acoust. Soc. Am. **94**, 1807(A) (1993).
[22] M. Facchinetti, ''Etude des vibrations de l'anche de la clarinette'' and ''Analisi del comportamento dinamico di un clarinetto,'' Ecole Polytechnique-Paris and Politecnico-Milano (1999).
[23] M. Facchinetti, X. Boutillon, and A. Constantinescu, ''Application of modal analysis and synthesis of reed and pipe to numerical simulations of a clarinet,'' J. Acoust. Soc. Am. **108**, 2590(A) (2000).
[24] E. Marandas, V. Gibiat, C. Besnainou, and N. Grand, ''Mechanical characterization of woodwind reeds,'' J. Phys. IV **4**, 633–636 (1994).
[25] E. Obataya and M. Norimoto, ''Acoustic properties of a reed (Arundo donax L.) used for the vibrating plate of a clarinet,'' J. Acoust. Soc. Am. **106**, 1106–1110 (1999).
[26] R.-J. Gibert, *Vibrations des Structures-Interactions avec les Fluides* (Eyrolles, Paris, 1988).
[27] K. Menou, B. Audit, X. Boutillon, and H. Vach, ''Holographic study of a vibrating bell: An undergraduate laboratory experiment,'' Am. J. Phys. **66**, 380–385 (1998).
[28] V. Gibiat and F. Laloe, ''Acoustical impedance measurements by the 2-microphone-3-calibration (tmtc) method,'' J. Acoust. Soc. Am. **88**, 2533–2545 (1990).
[29] V. Gibiat, ''Mesures d'impédance acoustique pour la clarinette,'' proprietary software and private communication, 1999.
[30] B. Gazengel, ''Caractérisation ... des instruments à anche simple'' (Characterization ... of simple reed instruments), Ph.D. thesis, Université du Maine-Le Mans, 1994.
[31] F. Pinard, B. Laine, and H. Vach, ''Musical quality assessment of clarinet reeds using optical holography,'' J. Acoust. Soc. Am. **113**, 1736–1742 (2003).